

Fast versus slow response in climate change: implications for the global hydrological cycle

Govindasamy Bala · K. Caldeira · R. Nemani

Received: 9 January 2009 / Accepted: 21 April 2009
© Springer-Verlag 2009

Abstract Recent studies have shown that changes in global mean precipitation are larger for solar forcing than for CO₂ forcing of similar magnitude. In this paper, we use an atmospheric general circulation model to show that the differences originate from differing fast responses of the climate system. We estimate the adjusted radiative forcing and fast response using Hansen's "fixed-SST forcing" method. Total climate system response is calculated using mixed layer simulations using the same model. Our analysis shows that the fast response is almost 40% of the total response for few key variables like precipitation and evaporation. We further demonstrate that the hydrologic sensitivity, defined as the change in global mean precipitation per unit warming, is the same for the two forcings when the fast responses are excluded from the definition of hydrologic sensitivity, suggesting that the slow response (feedback) of the hydrological cycle is independent of the forcing mechanism. Based on our results, we recommend that the fast and slow response be compared separately in multi-model intercomparisons to discover and understand robust responses in hydrologic cycle. The significance of this study to geoengineering is discussed.

1 Introduction

Recent studies (Allen and Ingram 2002; Andrews et al. 2009; Bala et al. 2008) have shown that the hydrologic sensitivity, defined as the percentage change in global-mean precipitation per degree is larger for solar forcing than for CO₂ forcing. Differences between CO₂ and solar radiative forcing of the troposphere (Allen and Ingram 2002), and radiative forcing at the surface (Bala et al. 2008) have been invoked to reconcile the differences in hydrologic sensitivity. Rapid adjustment of the troposphere in the solar case which reduces the effective radiative forcing by about 25%, and the absence of this adjustment for CO₂ case have been also cited as the primary reason for the differing hydrological sensitivity (Lambert and Faull 2007).

The fast response or rapid adjustment refers to the adjustment of the stratosphere, troposphere and the land surface before any change in global- and annual-mean surface temperature (ΔT) occurs. Fast adjustment in radiative fluxes is also referred to as the adjusted radiative forcing. The response that depends on ΔT is called the slow response or feedback and is usually represented as change in the specific variable per unit ΔT . For equilibrium climate change experiments using slab-ocean models forced by instantaneous radiative forcings, the simulated climate change actually represents the total climate change which is the sum of both fast and slow responses.

Recent investigations (Andrews and Forster 2008; Andrews et al. 2009; Gregory and Webb 2008) reveal that an elevated CO₂ causes significant rapid tropospheric adjustment leading to changes in cloud, water vapour, ice and snow, and reduction in effective radiative forcing. There are indications that tropospheric adjustment to CO₂ may be responsible for some of the model spread in equilibrium climate sensitivity and could affect time-dependent

G. Bala (✉)
Divecha Center for Climate Change & Center for Atmospheric and Oceanic Sciences, Indian Institute of Science, Bangalore 560012, India
e-mail: bala.gov@gmail.com

K. Caldeira
Department of Global Ecology, Carnegie Institution, 260 Panama Street, Stanford, CA 94305, USA

R. Nemani
NASA Ames Research Center, Moffett Field, Santa Clara, CA 94035, USA

climate projections (Gregory and Webb 2008). It has also been shown that the cloud feedback, defined as the part of the change that evolves with ΔT , is small and most of the cloud changes are fast adjustments.

A question then naturally arises whether the differences in rapid adjustments are responsible for the apparent difference in hydrologic sensitivity between CO_2 and solar forcings. For instantaneous doubling of CO_2 , the fast response involves reduction in surface evaporation and hence precipitation (Gregory and Webb 2008; Yang et al. 2003). This is because radiative forcing at the surface caused instantaneously by doubling of CO_2 is much smaller than that at the top of atmosphere (TOA) (Bala et al. 2008; Collins et al. 2006a; Hansen et al. 1997). Since the atmosphere has a relatively small heat capacity, it cannot store heat and hence the forcing differences between the surface and TOA must be eliminated on a time scale of few months. Therefore, non-radiative fluxes at the surface undergo rapid changes such that the net forcing at the surface and TOA are the same after the fast adjustment. A reduction in latent heat flux to the atmosphere (evaporation at the surface) and hence precipitation is a major part of this adjustment as shown in this study; reducing the later heat release in the troposphere (via precipitation process) helps to alleviate the CO_2 -heating gradient in the vertical. Since Bowen's ratio (ratio of sensible to latent heat fluxes) is about 0.2, it is likely that the latent heat response will dominate over sensible heat fluxes as it does in this study and in previous studies (Andrews et al. 2009; Bala et al. 2008). In the case of solar forcing, the gradient of the instantaneous radiative forcing in the vertical is much smaller (Hansen et al. 1997) and therefore, the reduction in latent heat flux and precipitation are expected to be small for the fast adjustment in this case.

The fast response of any climate variable can be estimated by regressing that variable against ΔT in instantaneous forcing experiments using climate models (Gregory et al. 2004); the intercept for $\Delta T = 0$ gives an estimate of the fast response. It can also be estimated by running a climate model with prescribed sea surface temperature (SST) and sea ice concentration (Hansen et al. 2005): by comparing simulations with and without the forcing, one can estimate the fast response. This method is referred to as Hansen's "fixed-SST forcing". The limitation of this method is that there will be a small climate change (ΔT is of the order of a few tenths of a degree) resulting from a change in land surface temperature. This limitation can be removed by also fixing the land surface temperatures (Shine et al. 2003) which is technically more difficult to do in a GCM. The slow response of any climate variable is usually obtained from the slope of the regression line for that variable in the regression method (Gregory et al. 2004): the fixed-SST forcing method cannot give the slow response.

In this study, we estimate both the fast and slow response to CO_2 and solar forcing in a climate model. The main goal is to show that the differences noted in the total response of the hydrological cycle arise from differences in the fast adjustments in the two cases. We further demonstrate that the slow response of the hydrological cycle which is a response to ΔT is about the same to CO_2 and solar forcings. It should be noted that a more recent study has reached a similar conclusion using UKMO-HadSM3 (Andrews et al. 2009). We believe that our paper should be considered as complementary to this recent study, not only because it confirms the idea with another model, but because it is investigated further with fixed-SST experiments which are particularly useful for analyzing the spatial patterns of fast response as demonstrated here.

2 Model and experiments

We use the community atmosphere model (CAM3.1) (Collins et al. 2006b) to investigate the differing response of hydrological cycle to CO_2 and solar forcings. The same model has participated in the multi-model intercomparison studies of fast responses to CO_2 forcing using the name "CCSM3.0" (Andrews et al. 2009; Gregory and Webb 2008) with a spectral T85 resolution. In this study, we use the "Finite Volume" transport method for the atmospheric dynamics. The horizontal resolution of the model for this study is 2° in latitude and 2.5° in longitude. There are 26 levels in the vertical. Two configurations for representing ocean and sea ice are employed: (1) prescribed sea surface temperatures (SST) and sea ice concentrations for estimating the fast adjustment, (2) a simple slab ocean-thermodynamic sea ice configuration for simulating the total response and hence for deriving the slow response. We performed three experiments using the first configuration with observed climatological SST and sea ice: (1) "Climo" simulation with an atmospheric CO_2 concentration of 355 ppmv (CO_2 level corresponding to year 1990) and a "solar constant" of $1,370 \text{ W m}^{-2}$, (2) " $2\times\text{CO}_2$ -climo" is similar to Climo but with the CO_2 concentration doubled to 710 ppmv, (3) "Solar-climo" is also similar to the Climo simulation but the solar constant is increased by 1.8% so that solar forcing is approximately close to the CO_2 forcing in the $2\times\text{CO}_2$ -climo case. Each of these prescribed SST simulations started on 1 September and lasted for 30 years and 4 months. The first 4 months are discarded when we assess climate statistics. These three experiments constitute the "fixed-SST forcing" (Hansen et al. 2005) method in our study to estimate the fast response of the climate system. Three additional experiments are performed using the second configuration with a slab ocean-thermodynamic sea ice model coupled to the same atmosphere model:

(4) “Control”, (5) “ $2\times\text{CO}_2$ ” and (6) “Solar” simulations with forcings as prescribed in the Climo, $2\times\text{CO}_2$ -climo, and Solar-climo cases, respectively. Each simulation lasts for 50 years, and the last 30 years are used for calculating climate statistics. The drift in global- and annual-mean surface temperature in the 30-year segment used for the analysis is of the order of 1×10^{-4} K. The first 20 years which is the time taken by the slab ocean model to reach equilibrium are discarded. Total response (slow plus fast response) of the climate system to CO_2 and solar forcings are calculated using these three experiments. We derive the slow response by subtracting the fast response (estimated by the fixed-SST method) from the total response. Differences in the fast and slow responses to CO_2 forcing between our study and the “CCSM3.0” model in Andrews et al. (2009) and Gregory and Webb (2008) are probably related to different resolutions ($2^\circ \text{ lat} \times 2.5^\circ \text{ lon}$ vs. $1.4^\circ \text{ lat} \times 1.4^\circ \text{ lon}$) and dynamical methods (finite volume vs. spectral).

3 Results

3.1 Estimation of adjusted forcing and fast response

The changes in global- and annual-mean values of key climate variables in $2\times\text{CO}_2$ -climo and Solar-climo relative to the Climo case are shown in Table 1. These changes (adjusted radiative forcing and fast adjustments of non-radiative fluxes) is also estimated using Gregory’s regression method (Gregory et al. 2004) applied to the slab-ocean experiments. It has been shown that there is good agreement between the fixed-SST method and regression analysis when the later is used with the first 10 years of simulation (Hansen et al. 2005). We have used 15 years for our regression analysis (Table 1) as discussed in Sect. 3.3. In general, the regression method tends to give more negative and less positive forcings (Gregory and Webb 2008) and the differences are statistically significant at the 5% level in many cases. The comparison of regression and fixed-SST methods is not the focus of this study but we do make a brief comparison of these methods in Sect. 3.3.

The “best” result of the regression method depends on the optimal number of years used in the analysis and hence uncertainty could be large. Specifically, the error in the estimation of intercept (fast response) could be large because there are few points near the intercept. The advantage of Hansen’s “fixed-SST forcing” method is that the adjusted forcing and fast adjustments can be evaluated to arbitrary precision by running a long enough experiment. The spatial patterns of fast adjustment are also directly available in the fixed-SST method. Therefore, we focus our discussion on the fixed-SST forcing method for estimating the fast adjustment in our study.

The fast adjustment leads to a land surface warming of 0.37 and 0.24 K in the $2\times\text{CO}_2$ -climo and Solar-climo cases, respectively (Table 1). Other climate models also simulate similar land surface warming (Andrews et al. 2009). After the fast adjustment, the surface and TOA forcing are the same since atmosphere does not store heat on time scales of more than a few months. While the TOA forcing is purely radiative, surface forcing consists of both radiative and non-radiative fluxes. Since the radiative components at the surface differ from that at TOA (Bala et al. 2008), changes in non-radiative fluxes (latent and sensible heat fluxes) are expected so that the net climate forcings are equal at the surface and TOA. The latent heat flux decreases in both the cases but the decreases are larger by about 1 Wm^{-2} in the $2\times\text{CO}_2$ -climo case compared to the Solar-climo case. Correspondingly, precipitation decreases in both the cases with larger decreases in the $2\times\text{CO}_2$ -climo case. The larger decrease in $2\times\text{CO}_2$ -climo is related to strong vertical gradient in longwave absorption by elevated CO_2 with stronger absorption in the upper troposphere and weaker absorption in the lower troposphere (Bala et al. 2008; Collins et al. 2006a; Hansen et al. 1997). This vertical gradient in long wave forcing can be seen from Table 1 which shows that the adjusted surface longwave forcing is about 1.7 Wm^{-2} lower than the forcing at TOA in the $2\times\text{CO}_2$ -climo case. The fast adjustments are also slightly different for the column precipitable water (Table 1) which is related to different fast responses in the stratosphere as we will see below. The adjustments in sensible heat fluxes are much smaller compared to that in latent heat fluxes.

It is important to note that the TOA and surface radiative forcings in the $2\times\text{CO}_2$ -climo and Solar-climo cases for both clear- and cloudy-sky (Table 1) include both the instantaneous radiative forcings and the fast response. For instance, the TOA cloudy-sky shortwave radiative forcing component for the solar experiment (-1.39 Wm^{-2}) does not arise from cloud adjustment alone. It is the sum of instantaneous radiative forcing component for cloudy-sky and fast cloud adjustment. The instantaneous shortwave radiative forcing for cloudy-sky is approximately estimated as $\text{SWCF} \times \Delta Q/Q = \sim -1.0 \text{ Wm}^{-2}$, where SWCF ($=-54.7 \text{ Wm}^{-2}$), Q ($=233.8 \text{ Wm}^{-2}$), are the shortwave cloud forcing, and TOA net shortwave absorption in the Climo simulation, and ΔQ ($=4.25 \text{ Wm}^{-2}$) is the instantaneous TOA shortwave forcing in the Solar-Climo case. ΔQ has been computed from

$$\Delta Q = \frac{\Delta\text{So}(1 - \alpha)}{4} \quad (1)$$

where ΔSo ($=25 \text{ Wm}^{-2}$) is the change in the solar constant in the Solar-climo case and α ($=0.32$) is the planetary albedo in the Climo simulation. Therefore, the TOA cloudy-sky

Table 1 Adjusted radiative forcing and fast response of non-radiative variables in the $2\times\text{CO}_2$ -climo, Solar-climo, $2\times\text{CO}_2$ and Solar cases

Variable	Fixed-SST method		Regression method	
	$2\times\text{CO}_2$ -climo	Solar-climo	$2\times\text{CO}_2$	Solar
TOA ^a clear-sky longwave radiative forcing ^b (Wm^{-2})	3.71 ± 0.15^c	-0.37 ± 0.15	3.80 ± 0.07	-0.42 ± 0.11
TOA cloudy-sky longwave radiative forcing (Wm^{-2})	-0.68 ± 0.11	-0.15 ± 0.11	-0.86 ± 0.18	-0.40 ± 0.17
TOA longwave radiative forcing ^d (Wm^{-2})	3.03 ± 0.15	-0.52 ± 0.20	2.94 ± 0.22	-0.81 ± 0.25
TOA clear-sky shortwave radiative forcing (Wm^{-2})	0.16 ± 0.11	5.45 ± 0.10	-0.23 ± 0.12	4.90 ± 0.18
TOA cloudy-sky shortwave radiative forcing (Wm^{-2})	0.18 ± 0.20	-1.39 ± 0.25	0.02 ± 0.40	-1.06 ± 0.43
TOA shortwave radiative forcing ^e (Wm^{-2})	0.34 ± 0.21	4.06 ± 0.28	-0.21 ± 0.40	3.84 ± 0.44
'Adjusted TOA radiative forcing' ^f (Wm^{-2})	3.37 ± 0.21	3.54 ± 0.20	2.73 ± 0.37	3.02 ± 0.46
Precipitation (%)	-1.80 ± 0.18	-0.7 ± 0.20	-0.87 ± 0.25	0.5 ± 0.34
Precipitable water (%)	0.7 ± 0.36	1.3 ± 0.30	2.27 ± 0.95	0.42 ± 0.54
Surface shortwave forcing ^g (Wm^{-2})	0.22 ± 0.22	2.49 ± 0.30	-0.33 ± 0.46	2.18 ± 0.51
Surface sensible heat forcing ^h (Wm^{-2})	-0.33 ± 0.13	-0.04 ± 0.10	-0.49 ± 0.15	-0.25 ± 0.15
Surface latent heat forcing ⁱ (Wm^{-2})	-1.46 ± 0.17	-0.52 ± 0.18	-0.63 ± 0.20	0.50 ± 0.28
Surface longwave forcing ^j (Wm^{-2})	1.34 ± 0.14	0.49 ± 0.21	1.67 ± 0.25	0.82 ± 0.38
Adjusted surface forcing ^k (Wm^{-2})	3.35 ± 0.24	3.54 ± 0.24	2.46 ± 0.36	2.75 ± 0.39
Land surface temperature change (K)	0.37 ± 0.18	0.24 ± 0.16	0	0
Global-mean surface temperature change (K)	0.17 ± 0.08	0.11 ± 0.07	0	0

^a Top of the atmosphere

^b Downward radiative fluxes provide positive forcing both at the surface and TOA

^c The uncertainty for each variable is ± 1 standard deviation estimated from a sample of 30 annual means in the fixed-SST method. For the regression method, the uncertainty is given by the standard error

^d TOA longwave radiative forcing is the sum of rows two and three

^e TOA shortwave radiative forcing is the sum of rows five and six

^f Adjusted TOA radiative forcing is the sum of rows four and seven

^g Incident minus reflected shortwave radiation at the surface

^h Upward sensible heat fluxes are positive

ⁱ Upward latent heat fluxes are positive

^j Downward minus upward longwave radiation at the surface

^k Adjusted surface radiative forcing is obtained by subtracting the sum of rows 12 and 13 from the sum of rows 11 and 14. Note that the surface forcing and TOA forcing are the same after tropospheric adjustment in the fixed-SST method since the atmosphere cannot store heat on time scales of more than a few months. However, this is not the case in the regression method

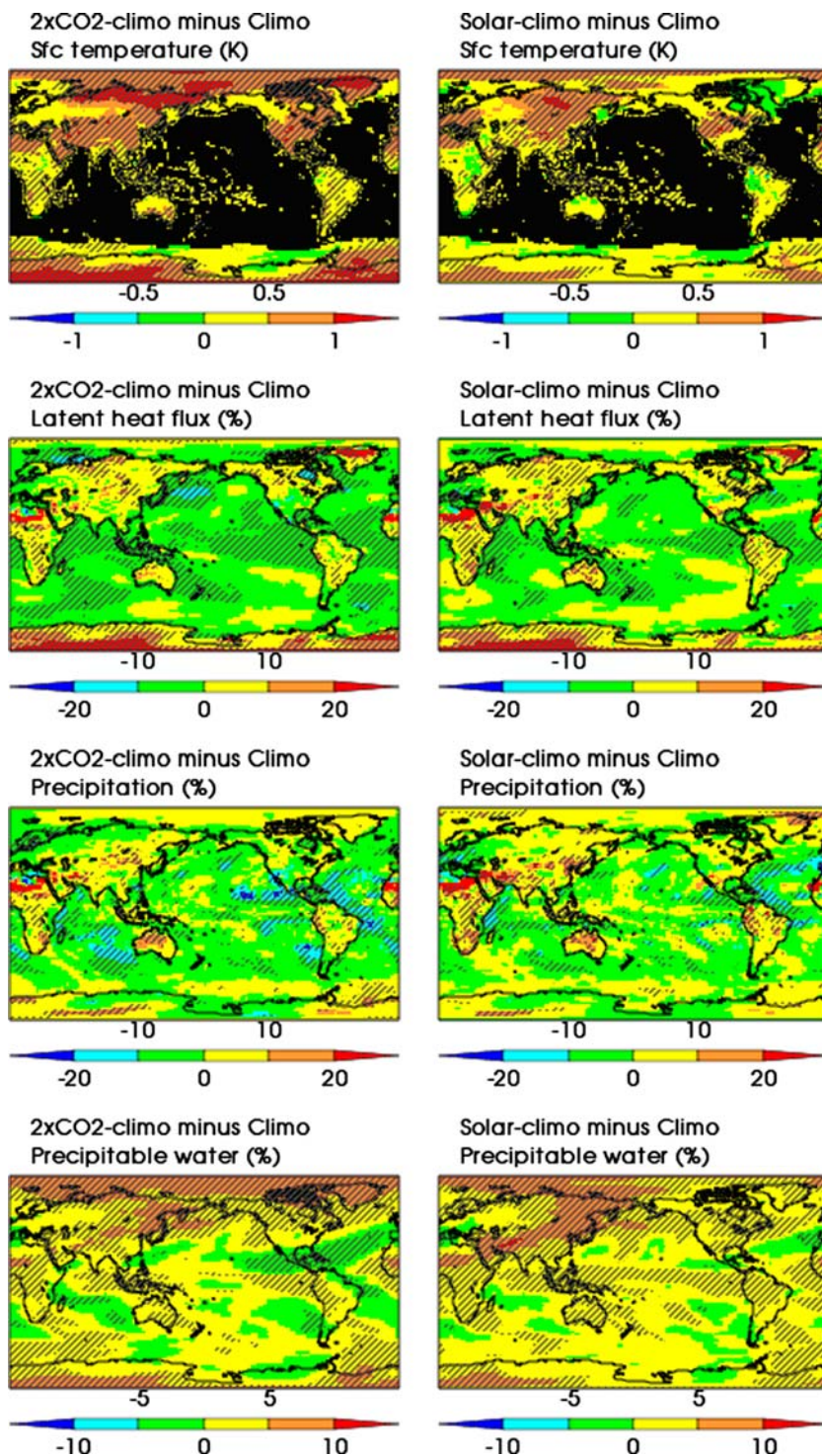
fast adjustment in shortwave is only $\sim -0.4 \text{ Wm}^{-2}$. Similar estimates for TAO clear-sky shortwave fluxes in the Solar-climo case yield an instantaneous forcing of $\sim 5.25 \text{ Wm}^{-2}$ and a fast response of $\sim 0.2 \text{ Wm}^{-2}$. An accurate estimation of fast responses for all the radiative fluxes would require separate calculation of the instantaneous radiative forcings which is beyond the scope of this study.

The spatial distribution of adjustment in surface temperature, evaporation, precipitation and precipitable water are shown in Fig. 1. The adjustment patterns are strikingly similar in the two cases but the magnitudes are enhanced in the $2\times\text{CO}_2$ -climo case for the surface temperature, evaporation and precipitation. Surface temperature over land and sea ice increases by more than 1°C in some locations (Fig. 1). A general decrease in precipitation and evaporation over the oceans and increases over land can be seen. Regional changes in evaporation and precipitation are of

the order of 10%. Regional water vapor changes are of the order of 5% with more positive changes in the Solar-climo case over the oceans.

Vertical distribution of the fast adjustments in temperature shows stratospheric cooling in the $2\times\text{CO}_2$ case and a slight warming in the Solar case (Fig. 2). These differences are related to enhanced longwave cooling in the stratosphere by elevated CO_2 in the $2\times\text{CO}_2$ -climo case and enhanced shortwave absorption by stratospheric ozone in the Solar-climo case. We notice larger changes in specific humidity in the Solar-climo case than in the $2\times\text{CO}_2$ -climo case which we believe is related to the warming in the stratosphere in the Solar-climo case. The pattern of fast adjustments in clouds in the $2\times\text{CO}_2$ -climo case (Fig. 2) shows mostly decreases in the troposphere which is in good agreement with other studies (Andrews and Forster 2008; Gregory and Webb 2008). There is a

Fig. 1 Fast adjustments in annual-mean surface temperature, latent heat flux (evaporation), precipitation, and precipitable water (column integrated water vapor) in the 2×CO₂-climo and Solar-climo cases. The *hatching* indicates regions where the changes are significant at the 1% level. Significance level is estimated using a Student's *t* test with a sample of 30 annual mean. For surface temperatures, fast adjustments can occur only over land and sea ice since sea surface temperature and sea ice concentration are prescribed. The spatial patterns of fast adjustments are similar in both cases but the magnitudes are different (Table 1): adjustments in surface temperature, latent heat flux and precipitation are larger for the 2×CO₂-climo case but precipitable water adjustment is larger in the Solar-climo case



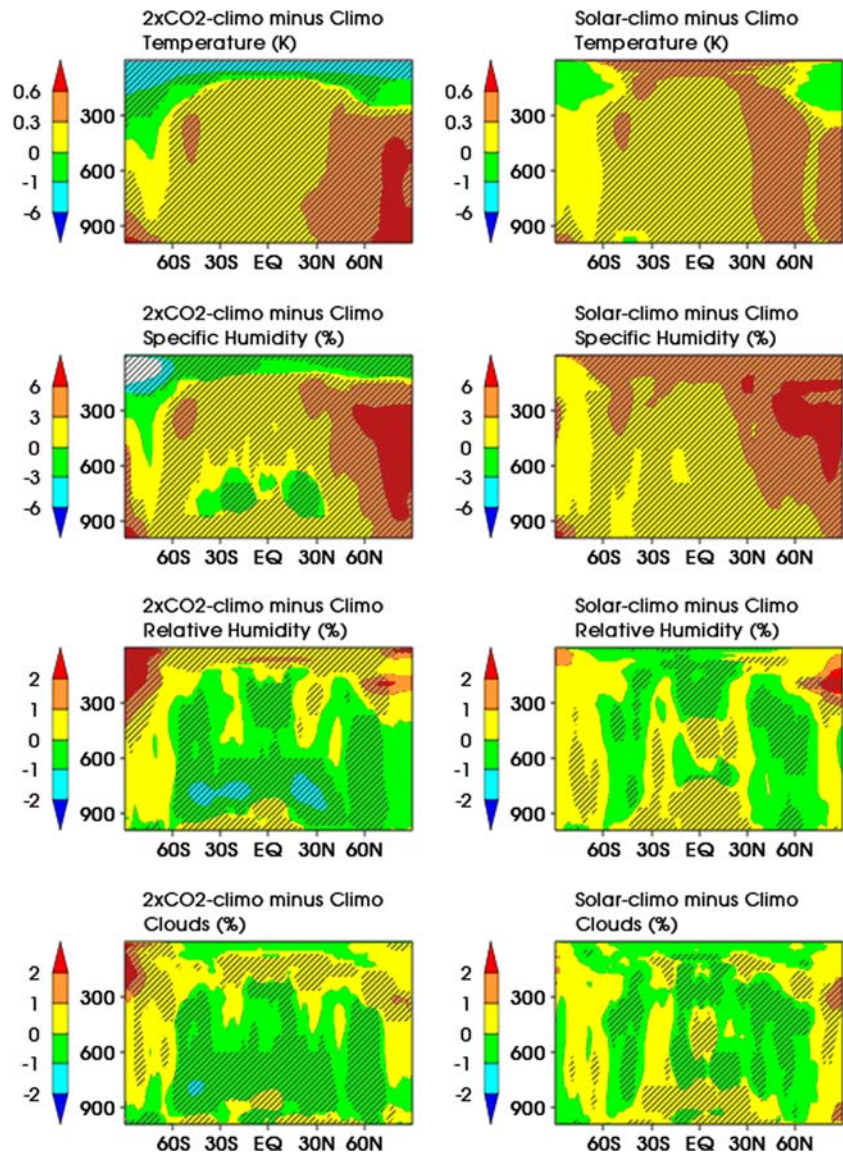
slight increase in the upper level clouds in the 2×CO₂-climo case. The fast cloud adjustment in the Solar-climo case slightly differs with some increases in the tropical lower troposphere. Unlike in the 2×CO₂ case, cloudiness decreases in the upper levels too. The cloud adjustment patterns in both the cases resemble the relative humidity adjustments, suggesting that the fast adjustments in

cloudiness are associated with relative humidity changes in this model.

3.2 Total and slow responses

Global- and annual-mean changes in 2×CO₂ and Solar relative to the Control are listed in Table 2. The surface

Fig. 2 Fast adjustments in zonal-mean temperature, specific humidity, relative humidity and cloud fraction in the $2\times\text{CO}_2$ -climo and Solar-climo cases. The *hatching* indicates regions where the changes are significant at the 1% level. Significance level is estimated using a Student's *t* test with a sample of 30 annual mean. To avoid errors due to interpolation, we did not perform any interpolation in the vertical and hence the *vertical axis* shown is the model's hybrid sigma coordinate. In general, the spatial patterns of adjustments are similar in both the cases with some exceptions: the stratosphere is colder in the $2\times\text{CO}_2$ -climo case while the Solar-climo shows a slight warming there, specific humidity increases everywhere in Solar-climo but it shows both increases and decreases in the $2\times\text{CO}_2$ -climo case. The patterns of fast adjustments in relative humidity and clouds resemble each other, suggesting that cloud changes are associated with relative humidity changes



temperature warms by 2.26 and 1.98 K in the $2\times\text{CO}_2$ and Solar cases, respectively. Land-mean warming is more than the ocean-mean warming in agreement with literature (IPCC 2007). Global-mean precipitation changes are 4.4 and 5.3%, respectively, and hence the hydrologic sensitivity as defined by the percentage change in precipitation per unit warming is 1.9 and 2.7% per K, respectively. This sensitivity is the total sensitivity that includes both the slow and fast responses (Allen and Ingram 2002; Bala et al. 2008; Held and Soden 2006; Wentz et al. 2007). This gives an impression that the hydrological sensitivity of the climate system strongly depends on the forcing mechanism. However, as we will show the hydrological sensitivity is almost independent of the forcing mechanism if we consider only the slow response, and fast response is excluded from climate change but included as part of the radiative forcing.

Table 2 Total climate response in $2\times\text{CO}_2$ and Solar cases

Variable	$2\times\text{CO}_2$	Solar
Global-mean surface temperature (K)	2.26 ± 0.36^a	1.98 ± 0.28
Land mean surface temperature (K)	2.50 ± 0.36	2.15 ± 0.29
Ocean mean surface temperature (K)	2.09 ± 0.36	1.86 ± 0.29
Global-mean precipitation (%)	4.39 ± 0.43	5.32 ± 0.42
Global-mean precipitable water (%)	15.27 ± 1.17	15.37 ± 1.04

^a The uncertainty for each variable is ± 1 standard deviation estimated from a sample of 30 annual means

To obtain the sensitivity due to slow response, we need to subtract the changes due to fast response estimated in the previous section. Consider a climate variable *x* whose total change is Δx_{tot} as simulated in the slab-ocean experiments. This total response can be decomposed into

Table 3 Slow climate response in $2\times\text{CO}_2$ and Solar cases using Eq. 5

Variable	$2\times\text{CO}_2$	Solar
Global-mean surface temperature (K)	2.09	1.87
Climate sensitivity (K/Wm^{-2})	0.62	0.53
TOA clear-sky longwave ($\text{Wm}^{-2} \text{K}^{-1}$)	-1.93	-2.01
TOA cloudy-sky longwave ($\text{Wm}^{-2} \text{K}^{-1}$)	0.23	0.17
TOA longwave ($\text{Wm}^{-2} \text{K}^{-1}$)	-1.70	-1.84
TOA clear-sky shortwave ($\text{Wm}^{-2} \text{K}^{-1}$)	0.84	0.78
TOA cloudy-sky shortwave ($\text{Wm}^{-2} \text{K}^{-1}$)	-0.68	-0.77
TOA shortwave ($\text{Wm}^{-2} \text{K}^{-1}$)	0.16	0.01
TOA net flux ($\text{Wm}^{-2} \text{K}^{-1}$)	-1.54	-1.83
Surface net shortwave ($\text{Wm}^{-2} \text{K}^{-1}$)	-0.55	-0.77
Surface net longwave ($\text{Wm}^{-2} \text{K}^{-1}$)	1.00	1.10
Surface sensible heat flux ($\text{Wm}^{-2} \text{K}^{-1}$; total response)	-0.37 (-0.35)	-0.35 (-0.49)
Surface latent heat flux ($\text{Wm}^{-2} \text{K}^{-1}$; total response)	2.41 (1.58)	2.59 (2.19)
Net surface energy flux ($\text{Wm}^{-2} \text{K}^{-1}$)	-1.59	-1.91
Hydrologic sensitivity ($\%/K$; total response) ^a	3.0 (1.94)	3.2 (2.69)
Precipitable water sensitivity ($\%/K$; total response)	7.0 (6.8)	7.5 (7.8)

^a Values in brackets show the total response that includes the fast adjustments

$$\Delta x_{\text{tot}} = \Delta x_{\text{f}} + \Delta x_{\text{s}} \quad (2)$$

where Δx_{f} and Δx_{s} are the fast and slow response components, respectively. The slow response is, therefore, obtained by subtracting the fast response (simulated in the fixed-SST experiments) from the total response simulated in the slab-ocean experiments. We separate the surface temperature response in a manner similar to Eq. 2:

$$\Delta T_{\text{tot}} = \Delta T_{\text{f}} + \Delta T_{\text{s}} \quad (3)$$

The fast response in temperature (which is confined to land) is only about 5–7% of the total response in our study (Tables 1, 2). However, the fast response in precipitation is about 40% of the total response in the $2\times\text{CO}_2$ case. Therefore, the separation of the fast and slow responses becomes important when we investigate the response of hydrological cycle to climate forcings. The sensitivity parameter for x , λ_x is usually defined as

$$\lambda_x = \Delta x_{\text{tot}} / \Delta T_{\text{tot}} \quad (4)$$

If we modify the definition of the sensitivity parameter so that it refers only to the slow response component, we have

$$\lambda_x = (\Delta x_{\text{tot}} - \Delta x_{\text{f}}) / (\Delta T_{\text{tot}} - \Delta T_{\text{f}}) \quad (5)$$

This definition basically represents the slope of the regression line in the Gregory's regression method (Gregory et al. 2004). The slow response of the various components of the climate system is computed using Eq. 5 and is listed in Table 3. The climate sensitivity, defined as the ratio of slow response in temperature to adjusted TOA radiative forcing (Table 1), is almost independent of forcing mechanism (Hansen et al. 1997): it differs between the two cases by only 20%. The responses of

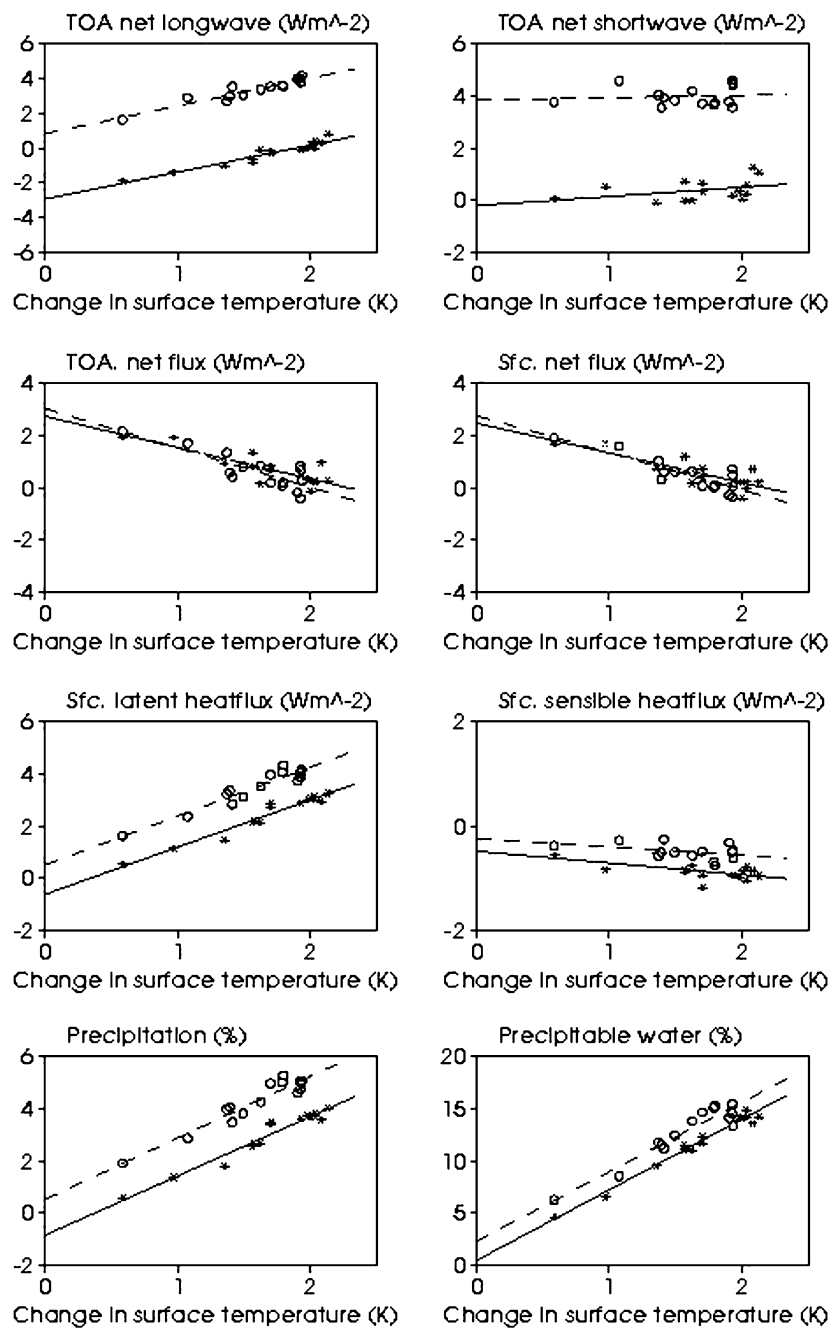
TOA clear-sky, and cloudy-sky components of shortwave and longwave fluxes and surface longwave responses differ by 10%. The surface shortwave radiative response differs by a larger 20%. The precipitation sensitivity is similar in the two cases when the fast response is excluded (Table 3). The slow response hydrologic sensitivity of 3% per unit warming is in good agreement with previous estimates of 2.8 (Andrews et al. 2009) and 3.4%/K (Allen and Ingram 2002) obtained from intercomparison of multiple models. The sensitivities of water vapor (precipitable water), sensible heat and latent heat fluxes are also nearly the same when the fast response is excluded.

3.3 Regression method

The slow response can be also obtained from the regression method (Gregory et al. 2004) (Fig. 3; Table 4). According to this method, the intercept of linear regression of any climate variable against ΔT gives the fast adjustment and the slow response (or feedback) is provided by the slope. There is some ambiguity in choosing how many points to perform the regressions on. We found that too much weight is given to the points at equilibrium if we use all the 50 annual-mean. Since the transient part of the integration will better constrains the regression line, the maximum number of points should be only 20 given the model takes ~ 20 years to reach equilibrium. After a few trials, we found that about 15 years worth of annual mean would suffice. Therefore, the regression analysis in this study (Tables 1, 4; Fig. 3) is performed using 15 years of data.

The slow response of TOA and surface fluxes, precipitation and water vapor (as represented by the slopes of the regression lines) are similar for climate change induced by

Fig. 3 Linear regression of TOA net longwave, shortwave, net radiative fluxes, surface net fluxes, surface latent and sensible heat fluxes, precipitation, and precipitable water against the global- and annual-mean surface temperature changes in the $2\times\text{CO}_2$ (stars and solid line) and Solar cases (circles and dashed line). The intercepts give estimates of the fast responses and the slopes yield the slow responses of the climate variables climate change. We can infer that the slow responses of all the variables shown are similar for climate change induced by both CO_2 and solar forcings. However, the intercepts are markedly different. In the case of radiative fluxes in the top panels, the differences are mainly caused by radiative forcings which act in different wavelengths; in longwave for the $2\times\text{CO}_2$ case and shortwave for the Solar case. Differing fast adjustments also partly contribute to the difference in the intercepts of radiative fluxes. However, differing fast adjustment is the sole driver for the differing intercepts for latent and sensible heat fluxes, precipitation and precipitable water



both CO_2 and solar forcings (Table 4; Fig. 3) suggesting that the slow responses are about the same, except for TOA cloudy sky shortwave and surface shortwave fluxes. The net feedback given by the slow response of the net TOA and surface forcings differ by about 20%. The differing shortwave responses mainly contribute to this difference in the slow response of net TOA and surface fluxes. The estimates of feedback parameters (Table 3) by subtracting the fast response from total response (Eq. 5) differ from the estimates from the regression method by (Table 4) about 10–20%.

The intercepts (Table 1; Fig. 3) are markedly different for TOA net longwave and shortwave fluxes mainly because the radiative forcings are in different wavelengths; in longwave for the $2\times\text{CO}_2$ case and shortwave for the Solar case. Differing fast adjustments also partly contribute to the difference in intercepts of radiative fluxes. However, fast adjustment is the sole driver for the differing intercepts in latent and sensible heat fluxes, precipitation and precipitable water.

It is instructive to note that the intercepts (Table 1; Fig. 3) which represent the adjusted radiative forcings and

Table 4 Slow climate response in $2\times\text{CO}_2$ and Solar cases from the regression method

Variable	$2\times\text{CO}_2$	Solar
TOA clear-sky longwave ($\text{Wm}^{-2} \text{K}^{-1}$) ^a	-1.82 ± 0.04^b	-1.88 ± 0.07
TOA cloudy-sky longwave ($\text{Wm}^{-2} \text{K}^{-1}$)	0.27 ± 0.10	0.28 ± 0.10
TOA longwave ($\text{Wm}^{-2} \text{K}^{-1}$)	-1.55 ± 0.10	-1.60 ± 0.15
TOA clear-sky shortwave ($\text{Wm}^{-2} \text{K}^{-1}$)	0.97 ± 0.07	1.04 ± 0.11
TOA cloudy-sky shortwave ($\text{Wm}^{-2} \text{K}^{-1}$)	-0.62 ± 0.23	-0.95 ± 0.26
TOA shortwave ($\text{Wm}^{-2} \text{K}^{-1}$)	0.35 ± 0.23	0.09 ± 0.27
TOA net flux ($\text{Wm}^{-2} \text{K}^{-1}$)	-1.20 ± 0.21	-1.51 ± 0.28
Surface net shortwave ($\text{Wm}^{-2} \text{K}^{-1}$)	-0.33 ± 0.27	-0.58 ± 0.32
Surface net longwave ($\text{Wm}^{-2} \text{K}^{-1}$)	0.78 ± 0.15	0.88 ± 0.23
Surface sensible heat flux ($\text{Wm}^{-2} \text{K}^{-1}$)	-0.22 ± 0.09	-0.16 ± 0.09
Surface latent heat flux ($\text{Wm}^{-2} \text{K}^{-1}$)	1.82 ± 0.12	1.88 ± 0.17
Net surface energy flux ($\text{Wm}^{-2} \text{K}^{-1}$)	-1.14 ± 0.21	-1.42 ± 0.24
Hydrologic sensitivity ($\% \text{K}^{-1}$)	2.28 ± 0.14	2.36 ± 0.21
Precipitable water sensitivity ($\% \text{K}^{-1}$)	6.78 ± 0.31	6.67 ± 0.58

^a Downward radiative fluxes provide positive forcing both at the surface and TOA

^b The uncertainty is given by the standard error from the regression

fast adjustments differ significantly from the estimates given by the fixed-SST method (Table 1). In general, we find that the regression method tends to give more negative and less positive forcings compared to fixed-SST method in agreement with an earlier study (Gregory and Webb 2008). For instance, the TOA net radiative forcings from the regression method are 2.73 and 3.02 Wm^{-2} for the $2\times\text{CO}_2$ and Solar cases but are 3.37 and 3.54 Wm^{-2} from the fixed-SST method. The sign of fast adjustments in precipitation and evaporation is negative (a positive surface forcing) in the fixed-SST method but positive (a negative surface forcing) for the Solar case and less negative for the $2\times\text{CO}_2$ case in the regression method.

The fixed-SST experiments require zero temperature change over all ice-free oceans while land areas are allowed to warm resulting in ΔT as shown in Table 1. However, the fast responses from regression require ΔT to be zero. This difference is likely to be part of the cause for the more positive forcings in the fixed-SST method than in the regression method: the small ΔT in the fixed-SST method results in an equivalent additional TOA radiative forcing ΔF (Hansen et al. 2005) given by

$$\Delta F = \Delta T_o / \lambda \quad (6)$$

where λ is climate sensitivity parameter and ΔT_o is the change in global- and annual-mean surface temperature change in the fixed-SST experiments. Equation 6 implies that the fixed-SST method will produce more radiative forcing than the regression method: using the values for ΔT_o (Table 1) and λ (Table 3), we find that this extra forcing explains about 0.2–0.3 Wm^{-2} , about 50% of the differences. The rest is attributable to the uncertainties in our estimations in both fixed-SST and regression methods (Table 1).

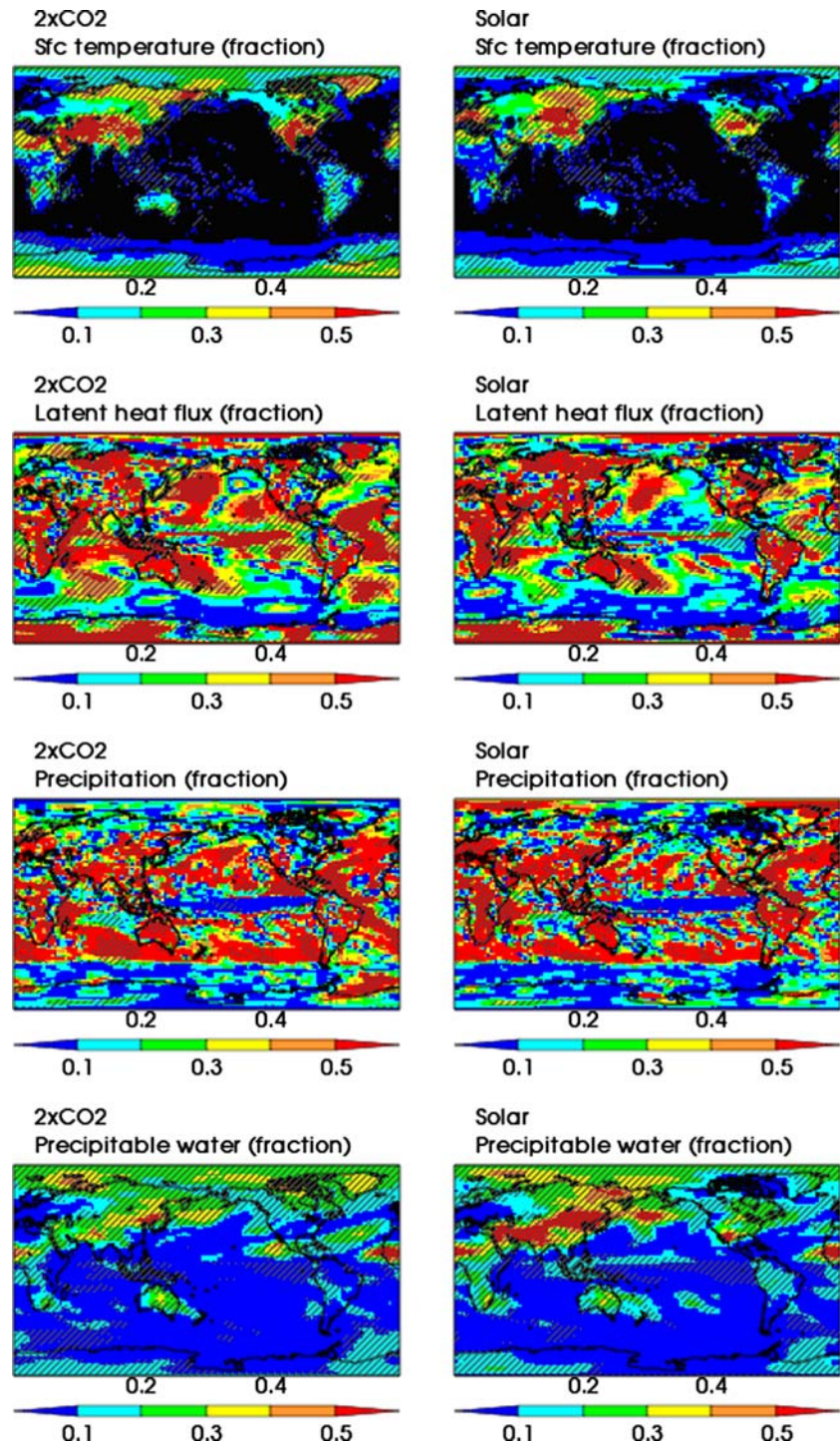
The spatial pattern of the ratio of the magnitude of fast response to the magnitude of the slow response shows that the fast response in land surface temperatures in some regions can be as high as 50% of the slow response (Fig. 4). This ratio is obtained by dividing the magnitude of the fast adjustment shown in Fig. 1 by the slow response which is obtained from Eq. 2. High fractional values over ocean and land areas are obtained for evaporation and precipitation, suggesting larger fraction for fast response in the hydrological cycle. The pattern for precipitable water is similar to the surface temperature, indicating very strong control of temperature on the water vapor field.

4 Discussion

In this study, we have investigated the fast response of climate system to CO_2 and solar forcings in detail. The fast response at the surface involves a reduction in evaporation for both the forcings which is mirrored as a reduction in precipitation. Therefore, instantaneous radiative forcing itself induces a response on a timescale of a few months to a year before the global- and annual-mean surface temperature changes. Since this fast response is almost 40% of the total response for a few key variables like precipitation and evaporation in the CO_2 -forcing case, it becomes important to separate the fast response from slow response that truly represents the feedbacks in the climate system. When the fast response component is subtracted from the total response, we are able to derive the slow response component. We find that this slow response or feedback is the same for CO_2 and solar forcing for the hydrological cycle.

Modeling and observational studies have estimated that the hydrologic sensitivity for CO_2 forcing is about

Fig. 4 Ratio of the magnitude of fast adjustment to the magnitude of slow adjustment for climate changes in $2\times\text{CO}_2$ and Solar cases. The *hatching* indicates regions where the fast adjustments are significant at the 1% level. Significance level is estimated using a Student's *t* test with a sample of 30 annual mean. There are regions where this fraction exceeds 0.5, suggesting that the magnitude of fast response is half the slow response in those regions. While fast adjustments in temperature and precipitable water are mostly confined to land areas, both land and oceanic areas show large fast adjustments in evaporation and precipitation



2%/K (Adler et al. 2008; Bala et al. 2008; Held and Soden 2006). However, as we have discussed before, this value represents the total response of the hydrologic cycle and is an underestimate of true hydrologic response because of the inclusion of the fast response. The slow response has higher value: $\sim 3\%/K$ as discussed in this paper, 2.8%/K for the ensemble average of CMIP-3 (the third coupled model intercomparison project) models

(Andrews et al. 2009) and 3.4%/K in CMIP2 models (Allen and Ingram 2002). Because the fast response could be as high as 40% of the total response and could vary among models, we recommend that the fast and slow response be compared separately when multi-model intercomparisons are made. Such separation may help us to discover and understand robust responses in hydrologic cycle.

Climate modeling studies have indicated that CO₂-fertilization reduces surface evaporation via increased “water efficiency” and hence can lead to surface warming and affect surface hydrology (Betts et al. 2007; Gedney et al. 2006; Levis et al. 1999, 2000; Matthews and Caldeira 2007; Sellers et al. 1996). Therefore, it is possible that part of the reduction in surface evaporation in our study is due to CO₂-fertilization of plants in the land model. To quantify this, we performed two additional experiments (one with prescribed SST and another with slab-ocean model) where the effects of increased CO₂ levels are seen by the land model but not by the radiative transfer model of the atmosphere. A mean warming of 0.1 K over the land surface, and negligible changes in the hydrological cycle were obtained for a doubling of CO₂ (Cao et al. 2009). The hydrological changes from CO₂-fertilization are one or two orders of magnitude smaller than the fast adjustments investigated in this paper. Therefore, the fast hydrological adjustments discussed in this modeling study are primarily driven by radiative forcing. It should be, however, noted that there is uncertainty in the quantification of the climate effects of CO₂-fertilization: while our modeling study finds negligible effect, another modeling study (Betts et al. 2007) simulated a CO₂-fertilization effect that is of the same order of magnitude as the fast adjustments simulated in this study.

How robust is our result that the hydrological response is different for solar and CO₂ forcing? A previous version (CCM3) of the model used here (Bala et al. 2008) and one other recent study using UKMO-HadSM3 model (Andrews et al. 2009) have shown similar results. The fast adjustments in precipitation in the UKMO-HadSM3 model, using the regression method, are -2.98 and -0.84% for the doubling CO₂ and an equivalent solar forcing, respectively. These reductions are quite large compared to -0.87 and $+0.5\%$ obtained in this study by the same regression method (Table 1). However, values obtained in the fixed-SST method (-1.80 and -0.70%) are quite comparable to the HadSM3 study. This suggests that while there is robustness in the sign of the differential hydrological response to CO₂ and solar forcings, the absolute values of the fast adjustment could vary among models. Additionally, there are significant differences between the fixed-SST and regression methods as noticed in this study and by Gregory and Webb (2008).

The main result, that the fast hydrological responses to solar and CO₂ forcing are different is related to the differential tropospheric absorption of energy to CO₂ and solar forcings. The differential absorption is simulated by column radiation models (Hansen et al. 1997) that are embedded within GCMs and hence the basic result does not have anything to do with the complexity of the GCMs. This is discussed in our earlier paper on this subject (Bala

et al. 2008). The differential absorption is also represented in radiative convective models (RCM). However, one cannot simulate the differential hydrological response in an RCM because changes in vertical profile of temperature and not precipitation are predicted by RCMs: the effect of convection is parameterized simply in the form of a fixed lapse rate and there is no precipitation physics in RCMs. We do believe that a single column model (SCM) which has parameterization for moist physics and radiative transfer should be able to simulate this differential hydrological response. We plan to perform SCM simulations in a future study.

A recent modeling study on sunshade geoengineering shows that insolation reductions sufficient to offset global-scale temperature increases lead to a decrease in global mean precipitation (Bala et al. 2008). This study concluded that solar forcing is more effective in driving changes in global mean evaporation than is CO₂ forcing of a similar magnitude and implied that an alteration in solar forcing might offset temperature changes or hydrological changes from greenhouse warming, but could not cancel both at once. Similar conclusions on reduced hydrological cycle in geo-engineered climate have been reached by other modeling studies on geoengineering (Lunt et al. 2008; Matthews and Caldeira 2007; Rasch et al. 2008; Robock et al. 2008). Our investigation in this paper provide insights into the cause for the differing hydrological changes between $2\times\text{CO}_2$ and solar forcings and concludes that the differing fast responses in the hydrological cycle are main cause for the differing hydrologic sensitivity.

Acknowledgments We thank Prof. J. Srinivasan and Drs. Karl Taylor and Peter Caldwell for their interest in this work and helpful discussions on fast adjustments induced by instantaneous CO₂ and solar forcings.

References

- Adler RF et al (2008) Relationships between global precipitation and surface temperature on interannual and longer timescales (1979–2006). *J Geophys Res Atmos* 113:D22103. doi:[10.1029/2008JD010536](https://doi.org/10.1029/2008JD010536)
- Allen MR, Ingram WJ (2002) Constraints on future changes in climate and the hydrologic cycle. *Nature* 419:224–232. doi:[10.1038/nature01092](https://doi.org/10.1038/nature01092)
- Andrews T, Forster PM (2008) CO₂ forcing induces semi-direct effects with consequences for climate feedback interpretations. *Geophys Res Lett* 35:L04802. doi:[10.1029/2007GL032273](https://doi.org/10.1029/2007GL032273)
- Andrews T et al (2009) A surface energy perspective on climate change. *J Clim* (in press)
- Bala G et al (2008) Impact of geoengineering schemes on the global hydrological cycle. *Proc Natl Acad Sci USA* 105(22):7664–7669. doi:[10.1073/pnas.0711648105](https://doi.org/10.1073/pnas.0711648105)
- Betts RA et al (2007) Projected increase in continental runoff due to plant responses to increasing carbon dioxide. *Nature* 448:1037–1041. doi:[10.1038/nature06045](https://doi.org/10.1038/nature06045)

- Cao L et al (2009) Climate response to physiological forcing of carbon dioxide simulated by the coupled Community Atmosphere Model (CAM3.1) and Community Land Model (CLM3.0). *Geophys Res Lett* (in press)
- Collins WD et al (2006a) Radiative forcing by well-mixed greenhouse gases: estimates from climate models in the Intergovernmental Panel on Climate Change (IPCC) Fourth Assessment Report (AR4). *J Geophys Res Atmos* 111:D14317
- Collins WD et al (2006b) The formulation and atmospheric simulation of the Community Atmosphere Model version 3 (CAM3). *J Clim* 19(11):2144–2161. doi:[10.1175/JCLI3760.1](https://doi.org/10.1175/JCLI3760.1)
- Godney N et al (2006) Detection of a direct carbon dioxide effect in continental river runoff records. *Nature* 439:835–838. doi:[10.1038/nature04504](https://doi.org/10.1038/nature04504)
- Gregory J, Webb M (2008) Tropospheric adjustment induces a cloud component in CO₂ forcing. *J Clim* 21(1):58–71. doi:[10.1175/2007JCLI1834.1](https://doi.org/10.1175/2007JCLI1834.1)
- Gregory JM et al (2004) A new method for diagnosing radiative forcing and climate sensitivity. *Geophys Res Lett* 31:L03205. doi:[10.1029/2003GL018747](https://doi.org/10.1029/2003GL018747)
- Hansen J et al (1997) Radiative forcing and climate response. *J Geophys Res Atmos* 102(D6):6831–6864. doi:[10.1029/96JD03436](https://doi.org/10.1029/96JD03436)
- Hansen J et al (2005) Efficacy of climate forcings. *J Geophys Res Atmos* 110:D18104
- Held IM, Soden BJ (2006) Robust responses of the hydrological cycle to global warming. *J Clim* 19(21):5686–5699. doi:[10.1175/JCLI3990.1](https://doi.org/10.1175/JCLI3990.1)
- IPCC (2007) *Climate change 2007: the physical science basis*. Cambridge University Press, Cambridge
- Lambert FH, Faull NE (2007) Tropospheric adjustment: the response of two general circulation models to a change in insolation. *Geophys Res Lett* 34:L03701. doi:[10.1029/2006GL028124](https://doi.org/10.1029/2006GL028124)
- Levis S et al (1999) Potential high-latitude vegetation feedbacks on CO₂-induced climate change. *Geophys Res Lett* 26(6):747–750. doi:[10.1029/1999GL900107](https://doi.org/10.1029/1999GL900107)
- Levis S et al (2000) Large-scale vegetation feedbacks on a doubled CO₂ climate. *J Clim* 13(7):1313–1325. doi:[10.1175/1520-0442\(2000\)013<1313:LSVFOA>2.0.CO;2](https://doi.org/10.1175/1520-0442(2000)013<1313:LSVFOA>2.0.CO;2)
- Lunt DJ et al (2008) “Sunshade World”: a fully coupled GCM evaluation of the climatic impacts of geoengineering. *Geophys Res Lett* 35:L12710. doi:[10.1029/2008GL033674](https://doi.org/10.1029/2008GL033674)
- Matthews HD, Caldeira K (2007) Transient climate-carbon simulations of planetary geoengineering. *Proc Natl Acad Sci USA* 104(24):9949–9954. doi:[10.1073/pnas.0700419104](https://doi.org/10.1073/pnas.0700419104)
- Rasch PJ et al (2008) Exploring the geoengineering of climate using stratospheric sulfate aerosols: the role of particle size. *Geophys Res Lett* 35:L02809. doi:[10.1029/2007GL032179](https://doi.org/10.1029/2007GL032179)
- Robock A et al (2008) Regional climate responses to geoengineering with tropical and Arctic SO₂ injections. *J Geophys Res* 113:D16101. doi:[10.1029/2008JD010050](https://doi.org/10.1029/2008JD010050)
- Sellers PJ et al (1996) Comparison of radiative and physiological effects of doubled atmospheric CO₂ on climate. *Science* 271(5254):1402–1406. doi:[10.1126/science.271.5254.1402](https://doi.org/10.1126/science.271.5254.1402)
- Shine KP et al (2003) An alternative to radiative forcing for estimating the relative importance of climate change mechanisms. *Geophys Res Lett* 30:2047. doi:[10.1029/2003GL018141](https://doi.org/10.1029/2003GL018141)
- Wentz FJ et al (2007) How much more rain will global warming bring? *Science* 317(5835):233–235. doi:[10.1126/science.1140746](https://doi.org/10.1126/science.1140746)
- Yang FL et al (2003) Intensity of hydrological cycles in warmer climates. *J Clim* 16(14):2419–2423. doi:[10.1175/2779.1](https://doi.org/10.1175/2779.1)